

The impact of polymer selection and dose on the incorporation of ballasting agents onto wastewater aggregates

Olga Murujew¹, Jordan Geoffroy¹, Emeline Fournie¹, Elisa Socionovo Gioacchini¹, Andrea Wilson^{2,3}, Peter Vale², Bruce Jefferson¹, Marc Pidou^{1*}

¹Cranfield University, College Road, Cranfield, Bedfordshire, MK43 0AL, UK

²Severn Trent Water, 2 St Johns Street, Coventry, CV1 2LZ, UK

³Atkins Global, Woodcote Grove, Epsom, Surrey, KT18 5BW, UK

*Corresponding author: m.pidou@cranfield.ac.uk

Abstract

Ballasted flocculation is an efficient high-rate sedimentation process getting more attention as an advanced P removal technology for levels below 0.1 mg/L. The process is well-known yet only very few studies have investigated the interactions, within the matrix of wastewater, of coagulant, polymer and ballast, especially when it comes to polymer doses and types which are, in the industry, rather based on recommendations than scientific evidence. In this work, the impact of anionic and cationic polymers has been investigated on P removal and floc properties. Anionic polymers showed to be superior to cationic ones when it comes to P removal and doses even as low as 0.01 mg/L yield better results than coagulant alone. There appears to be a “best-case” floc size with which very good P removal (>90%) can be achieved and flocs of sufficient strength can be generated.

Keywords: polymer, phosphorus removal, magnetite, ballasted flocculation

1. Introduction

Established approaches to manage phosphorus concentrations in wastewater use either enhanced biological phosphorus (P) removal (EBPR), or more commonly, chemical precipitation (Yeoman et al., 1988). In Europe, the resultant final effluent concentration typically ranges between 1 and 2 mg P/L. The situation is changing with increasing numbers of sites requiring to further lower their effluent P concentration to below 1 mg P/L and potentially as low as 0.1 mg P/L (EU Water Framework Directive, 2000). Chemical P removal is undertaken through the addition of a metal salt (e.g. FeCl_3) to wastewater prior to either the primary or secondary treatment stage to precipitate the available phosphorus into aggregates which can then be easily removed from the water. P concentrations below 1 mg P/L can be achieved by increasing the amount of coagulant used, but very large doses are then required. The alternative is to dose ahead of a tertiary solid-liquid separation process with current examples including depth sand filtration, drum cloth filtration and ballasted flocculation. In such cases, doses of 4 mg/L to 15 mg/L as Fe have been reported for full-scale operations, generating a significant saving in total chemical usage (at least 20%) compared to increasing the dose at earlier stages in the treatment train (Bratby, 2016; Hook and Ott, 2001; Ragsdale, 2007).

In the United States of America, ballasted flocculation -a high-rate sedimentation process- has been shown to achieve very low effluent P concentrations (<0.1 mg P/L) which makes it an interesting technology for the current European context (De Barbadillo et al., 2010; Lee et al., 2015). In this process, phosphorus precipitation is first achieved by reaction with a coagulant followed by flocculation through the addition of ballasting agent and polymer which will directly influence flocs characteristics and settleability and lead to enhanced removal. Indeed, the inclusion of a ballasting agent such as sand or magnetite into the flocs significantly enhances their settling rate enabling removal in high rate clarification setups characterised by surface overflow rates of $33.6\text{--}80\text{ m}^3/\text{m}^2/\text{h}$ (De Barbadillo et al., 2010; Imasuen et al., 2004; Lee et al., 2015). The ballast is typically recycled to reduce costs and sludge production by passing the collected sludge through a hydrocyclone (Desjardins et al., 2002; Gasperi et al., 2012; Imasuen et al., 2004). In the

case of magnetite (Fe_3O_4), the hydrocyclone is followed by a magnetic drum to recover and recycle the ballast (Anderson and Priestley, 1983).

A polyelectrolyte is added to ensure the ballasting agent is incorporated within the floc structure and for the process works efficiently (Bolto et al., 1996; Jarvis et al., 2009). The polymers used are usually characterised by their molecular structure, molecular weight (MW) and charge density (CD) and work under three potential and simultaneous mechanisms: bridging, charge neutralisation and polymer adsorption (Bolto and Gregory, 2007; Rabiee, 2010). Accordingly, polymers may be uncharged, similarly (anionic) or oppositely charged (cationic) to the negatively charged particles in wastewater. Current recommendations in the industry concerning the implementation of the system are agnostic to polymer selection although cationic polymer has been suggested at a dose of 1 mg/L coupled to a coagulant dose of 8 mg/L. However, in some regions of the world, such as the UK, cationic polymers are discouraged by the local environment agency raising questions as to which polymers are most appropriate and what dose level should be applied as indeed previous studies on flocculation have highlighted the importance of polymer characteristics such as structure, charge and stability (Lapointe and Barbeau, 2019; Sharma et al., 2006). Previously reported trials of ballasted flocculation utilised a FeCl_3 coagulant dose of 14 mg/L and an anionic polymer^a dose of 1 mg/L to achieve a P reduction from 0.22 mg/L to 0.031 mg/L Total P during a four-week trial (De Barbadillo et al., 2010). Similarly, a pilot trial treating 11 m³/h of real wastewater with an initial P concentration of 1 mg TP/L achieved a final concentration of 0.025-0.039 mg TP/L with coagulant doses between 12-24 mg/L^b and a polymer dose of 0.7 mg/L (Lee et al., 2015). However, these trials are based on validating the ability to meet very low P concentrations rather than optimising dose requirements such that further savings are posited. To fully optimise the system, it is critical to understand the roles of the ballast and polymers. A number of studies have investigated ballasted floc formation, with in particular Ghanem et al. (2007) describing the incorporation of the ballasting agent within the floc by inertial forces rather than acting as seed material. Lapointe and Barbeau (2018) demonstrated, by studying a range of ballasting agents, the importance of surface interactions between the flocs and ballast and hence the critical role the surface characteristics of the ballasting agent play in floc formation. Lapointe

and Barbeau (2016) also defined optimum bench scale mixing conditions and polymer and ballasting agent dosages through a detailed study of ballasted flocs in both surface water and wastewater at microscopic level. However, there are very few studies available on the impact of polymer choice on the ballasted flocculation process with mainly the comparison of synthetic (polyacrylamide) and natural (starch) polymers (Lapointe and Barbeau, 2019). A previously published study demonstrated that the inclusion of the ballast reduced coagulant demand by a factor of ten whilst still increasing COD removal by a factor of five compared to a non-ballasted system (Imasuen et al., 2004). However, there remains no clear basis for selection of the type and dose of polymers in such systems. The current paper resolves this by examining the performance of seven different polymers in terms of both removal and resultant floc properties to inform a guide to selection for use in tertiary P removal systems.

^a Anionic polyacrylamides of very high MW and low CD.

^b Three coagulants were used: Alum: 12 mg/L, PACl: 20 mg/L, FeCl₃: 24 mg/L.

2. Materials and Methods

2.1. Materials

Wastewater was taken from a sewage works in the UK that has no primary treatment and utilizes oxidation ditches as secondary treatment. The site was being utilised as part of a large-scale demonstration trial of tertiary P removal technologies such that the samples were withdrawn from within the sampling points of the trials (Table 1). The P concentration was maintained at approximately 1 mg/L throughout by addition of KH₂PO₄ (Sigma-Aldrich, Dorset, UK) where required.

Ferric chloride (FeCl₃, 60% w/w) was used as coagulant, magnetite was used as ballast and, in total, seven polymers were tested. The magnetite, with a composition of 86-99% Fe₃O₄, had a density of 4.6-5.1 kg/L and d₅₀ of 64 ± 4 µm when dispersed in the wastewater. The polymers were all polyacrylamides and were chosen to have a wide range of characteristics (Table 2).

2.2. Methods

2.2.1. Jar test procedures

Experiments on P removal were performed with jar tests (Phipps & Bird, Richmond, Virginia, USA) with a standard and ballasted jar test methods. The standard method was used when tests with coagulant only (Co) were done. The procedure consisted of 2 minutes stirring at 200 rpm (corresponding to an average velocity gradient G of 128 s^{-1}) at the point of coagulant addition followed by 15 minutes stirring at 30 rpm ($G = 7.4 \text{ s}^{-1}$) and finalised by 30 minutes of settling. The ballasted jar test method was used when experiments with ballast alone (B), coagulant and ballast (CB), polymer and ballast (BP) and the full ballasted flocculation system (BCP) were performed simulating the conditions in real systems. At the point of coagulant addition, the mixture was stirred at 200 rpm for 2 minutes. After that, magnetite (ballast) was added at a dose of 5 g/L with mixing at 200 rpm for 1 minute followed by polymer addition and again stirring at 200 rpm for 1 minute. At the end, the mixture settled for 5 minutes. The mixing conditions, dosing sequence and times used were selected to replicate the conditions in a full scale commercial system. For the tests with B, CB and BP, the times were maintained but only the relevant components were added to the jars. For selected jar tests, pre-treated magnetite was used to simulate used ballast. This was prepared by stirring unused (fresh) magnetite in wastewater for 1 hour followed by drying at 105°C .

2.2.2. Water analysis

Ortho-phosphate was measured following a standard colorimetric method using cell tests (Hach, Sheffield, UK and Merck, Nottingham, UK). Turbidity was measured using a turbidimeter (Model 2100N, Hach, Sheffield, UK). Floc growth and properties were analysed with a particle size analyser (Malvern Mastersizer 3000, Malvern, UK). Floc strength (FS) was calculated according to:

$$FS = \frac{d_{stable}}{d_{peak}}$$

with d_{stable} : floc size at 60 minutes and d_{peak} : peak floc size.

2.2.3. Polymer characterisation

Viscosity of polymers was measured with a viscometer (Brookfield DV-E, Ametek, Harlow, UK) with the concentrations of the polymers adjusted to 0.5% and measurements done over a range of spindle rotation speeds between 0-100 /s. Zeta potential was measured using a Malvern Zetasizer (Nano Series, Nano ZS, Malvern, UK). The polymers were diluted in DI water to obtain a solution of 1 mg/L and the pH was then adjusted between 2 and 12 using HCl and NaOH. Structural analysis of polymers was done with Attenuated Total Reflection Fourier-transform infrared spectroscopy (ATR-FTIR) and nuclear magnetic resonance (NMR). Prior to FTIR scanning, the polymers were dried, dissolved in chloroform and then cast into a film on potassium bromide plates. The FTIR spectra were obtained in a region of 4000-650 cm^{-1} with a single scan per spectrum (Perkin Elmer Spectrum 100). For NMR measurements, polymers were dried and dissolved in deuterated water (D_2O) with trimethyl-silyl (TSP) agent. ^{13}C NMR spectra were obtained with composite pulse with ^1H decoupled and a 30° pulse (8.2 ms) with a pulse delay of 3 seconds applied (Bruker Avance II 300MZ NMR spectrometer with QNP probe).

3. Results and Discussion

3.1. Impact of polymer choice and dose on P removal

Phosphorus removal varied between 88% and 98% when using the seven different polymers in conjunction with coagulant and ballast (Figure 1). Three anionic (A1, A2 and A4) and one cationic polymer (C3) achieved the maximum recorded removal which corresponded to residual phosphorus concentrations below the level of detection of the analytical method (0.05 mg/L). In comparison, the other polymers achieved lower removal levels at 91%, 89% and 88% for polymers C1, C2 and A3, respectively. The other observable difference between the polymers relates to the kinetics of removal where polymers C3, A1 and A4 achieved their maximum removal within 30 seconds as opposed to between 3-5 minutes for the other polymers. In contrast, the use of coagulant only resulted in a significantly slower overall process and a lower final removal (Figure 1). To illustrate, phosphorus removal was 14.8%, 50.9% and 72.9% after 5, 15 and 30 minutes,

respectively. The significantly faster kinetics in the case of the polymers is congruent with previous trials in drinking water production and highlights the impact of the ballasting agent (Dixon, 1991). To elucidate the role of the polymer, a series of jar tests were conducted utilising the different components that make up the combined system using polymer A1 (Figure 2). Phosphorus removal for coagulation only (Co), ballast only (B), coagulant and ballast (CB) and ballast, coagulant and polymer (BCP) were 94%, 8%, 70% and 98%, respectively, when using 8 mg/L of coagulant as the pH remained relatively stable between 7.08 and 7.47 for all condition tested. Interestingly, phosphorus removal was found to be greater with coagulation alone than when combining coagulant and ballast. These results suggest that the ballast interfered with the coagulant reaction and affected its ability to target phosphorus. However, the full system combining coagulation, ballast and polymer achieved excellent phosphorus removal to very low levels (<0.05 mg/L). Decreasing the coagulant dose to 5 mg/L decreased P removal for the coagulation system only to 86% but increased removal for the CB system to 86%. However, in the BCP case, the removal was not impacted by lowering the coagulant dose by 38% offering a potential for substantial chemical savings. Again, pH remained relatively stable with values between 7.15 and 7.48 for all conditions tested.

A second series of trials were conducted with two anionic (A1 and A2) and two cationic polymers (C1 and C2) to further explore the role of the polymer by comparing its use alone (P) in conjunction with the ballast (BP), the coagulant (CP) or both (BCP) (Figure 3). Comparison of the phosphorus removal achieved with the four polymers when used alone (P) revealed that none of the polymers were effective as a primary precipitating agent (Figure 3). To illustrate, when used alone phosphorus removals of 34%, 7%, 3% and 1% were observed for polymers A1, A2, C1 and C2, respectively.

Combining the polymer with the ballast switched the sequence of efficacy of the polymers with the two cationic polymers being more effective with phosphorus removal levels of 44% and 69% for C1 and C2, respectively. In contrast, the anionic polymers, A1 and A2 resulted in phosphorus removal levels of 14% and 22%, respectively. Significantly improved removal was observed when

the polymer was used in conjunction with a ferric coagulant with phosphorus removal levels of 28-36%, 77-84%, 46-55% and 39-76% for A1, A2, C1 and C2, respectively. Interestingly, the removal with coagulant alone is higher than in conjunction with polymer suggesting the polymer is either inhibiting precipitation or is exerting a demand on the coagulant irrespective of its charge. Further, improved removal was observed when the coagulant dose was increased from 5 mg/L to 8 mg/L yielding an improvement in removal efficiency between 7-9% for A1, A2 and C1 with a much greater enhancement with C2 of an additional 37% phosphorus removal. When all components (BCP) were added to the process very high phosphorus removal (97.7%) was achieved with A1 and A2. This demonstrates that the ballasted flocculation process is more efficient than coagulation alone and enables very low residual phosphorus levels to be achieved. However, this observation only applies to the two anionic polymers tested (A1, A2) as reduced performance was observed for C1 and C2 such that it was comparable to coagulation alone at 87-92% as BCP compared to 86-95% when just using coagulant. No discernible impact was observed when reducing the polymer dose from 1 mg/L down to 0.3 mg/L with all four polymers at both 5 mg/L and 8 mg/L of coagulant and with fresh or reused ballast (Figure 4). In the case of the two anionic polymers and a coagulant dose of 8 mg/L, no impact was seen when reducing the polymer dose down to the lowest level tested, 0.01 mg/L or a 99% saving in polymer. When using the lower coagulant dose of 5 mg/L, a different profile was observed whereby the removal increased as a function of polymer doses up to around 0.3 mg/L. To illustrate, in the case of A1, phosphorus removal increased from 80% at 0.01 mg/L to 95.7% at 0.3 mg/L and then to 98% at 1 mg/L. Equivalent variation in removal was observed with the other three polymers at polymer doses below 0.3 mg/L but all systems then delivered stable removal irrespective of dose (Figure 4).

3.2. Impact of polymer choice and dose on floc size

For all polymers, the floc growth profiles followed a pattern of rapid growth reaching a peak size after 4-5 minutes followed by gradual decline until a steady state floc size was established (Figure 5). The choice of polymer has a significant impact on the maximum floc size achieved, the rate of

erosion and hence the time taken to reach a stable floc size. For instance, the maximum d_{50} floc size was 274 μm , 737 μm , 866 μm and 1443 μm for polymers C2, A1, C1 and A2, respectively. After 60 minutes all flocs had stabilised to similar size with a d_{50} between 165 and 197 μm (Figure 5). However, the rate of breakage was significantly different with the d_{50} floc size reaching 40% of its difference between peak and final size within 12, 18 and 45 minutes for polymers C1, A2 and A1, respectively. The flocs produced with polymer C2 were the smallest, eroded at a slower rate and decreased in total only by 41% compared to the others which decreased in size by 73-86%. Interestingly, polymer C1 showed a different breakage pattern to the others with a much greater initial fragmentation breakage profile (Jarvis et al., 2005a). To illustrate, the d_{50} floc size decreased by 499 μm in the 3 minutes after the peak value was observed, equivalent to a 58% reduction in the floc size. In comparison polymers C2, A1 and A2 decreased by 27 μm , (10%), 84 μm (11%) and 107 μm (7%) in the same time. In comparison, when coagulant alone is used, the flocs grow to a stable d_{50} size of approximately 610-600 μm for a period of 30 minutes before gradually eroding to a final size of between 510-530 μm . Accordingly, inclusion of polymer significantly impacts on the formation and breakage profiles of the flocs. This is illustrated through their respective floc strength factors of 0.14, 0.19, 0.26 and 0.59 for polymers A2, C1, A1 and C2 compared to coagulation alone with a floc strength factor of 0.83. A tendency for increasing floc strength factors with decreasing d_{50} peak floc sizes and with slower breakage rates can be seen for all polymers. This indicates that there may be an equilibrium size for the BCP system at which the flocs are big enough for very good P removal while producing large enough flocs of sufficient strength.

An increase in polymer dose resulted in an increased floc size in all cases (Table 3, Figure 6). To illustrate, in the case of polymer A1, the d_{50} floc size increased from 68.3 μm at a polymer dose of 0.01 mg/L to 154.3 μm , 413.7 μm and 337.0 μm at polymer doses of 0.1, 0.5 and 1 mg/L, respectively (Figure 6). This equates to a size increase factor of 4.9 between the low and high doses. Similar trends were observed for the other polymers with equivalent size increase factors of 10.9, 15.2 and 3.5 for polymers A2, C1 and C2, respectively. The impact in dose appeared to be more sensitive for the anionic polymer where a change in dose from 0.01 to 0.1 mg/L resulted in a

226% increase in the d_{50} for A1 and a 346% increase for A2. In comparison, an increase in d_{50} of 127% and 112% was measured for the cationic polymers C1 and C2. In all cases, the increased polymer dose generated more open, dendritic structures as evidenced by the change in the fractal dimension. To illustrate, in the case of the polymer A1, the fractal dimension decreased from a value of 2.7 at a polymer dose of 0.01 mg/L to 2.6, 2.2 and 2.3 for polymer doses of 0.1, 0.5 and 1.0 mg/L, respectively. Similar changes occurred with the other polymers except for C1 where the shape of the flocs remained more stable across the polymer doses tested.

The impact of polymer dose was further elucidated by comparing the particle size distributions at the peak size (roughly 4 minutes) and after 60 minutes to explore how the flocs break (Figure 7). Comparison of the PSDs for low doses revealed that the shape of the size distribution remained similar and that only a small shift in the size was observed congruent with an erosion mechanism dominating as is common with small flocs (Jarvis et al., 2005b). This was seen in the case of polymers A2, C1 and C2 with shifts in the mode size from 68.1 μm to 47.5 μm for A2, 56.5 μm to 45.6 μm for C1 and 61.2 μm to 55.5 μm for C2 (Figure 7). In the case of the higher polymer dose a different response can be seen where larger scale shift in particle size distribution can be observed which is more indicative of a fragmentation mechanism that occurs with large flocs that are bigger than the Kolmogorov scale of turbulence (Jarvis et al., 2005b). Previous research using similar jar testers have estimated the size of the turbulent eddies to be of a similar size to the flocs at the energy dissipation rate being used (Jarvis et al., 2005b). Accordingly, flocs bigger than this size are more likely to fragment. This is seen in the case of polymers A1, A2 and C1 but not C2. For instance, the mode size decreased from 782 μm to 199 μm when using 1 mg/L of A1 and from 1673 μm to 288 μm when using A2. In contrast the mode size changed from 322 μm to 178.7 μm when using 1 mg/L of C2. The impact of the polymer dose can also be considered in terms of the colloids by examining the d_{10} and the residual turbidity at the end of the settling phase (Table 3). Both data sets indicate a coherent observation in that higher doses increase the d_{10} floc size and reduce the residual turbidity. For instance, in the case of the anionic polymers the d_{10} size increased from 31.1 μm to 69.0 μm for A1 and 27.2 μm to 75.9 μm for A2 as the polymer dose increased from 0.01 to 1.0 mg/L. The corresponding residual turbidity were from 1.8 to 0.9 NTU for

A1 and from 1.7 to 0.7 NTU for A2. Whilst the same pattern was observed with the cationic polymers the d_{10} floc sizes were larger but the residual turbidity were higher indicating that either the polymers were less effective at capturing colloids or more breakage was occurring that generated fine particles. The evolution of the d_{10} floc size showed a sharp increase to a peak at 5 minutes with a steady decrease to a stable size at the end. Therefore, it suggests that the more likely explanation is that of greater fines generation during erosive floc breakage. Similarly, as with d_{50} , higher polymer doses resulted in larger flocs which then break down more quickly the larger the peak size was. From a treatment point of view, a linear regression ($R^2 = 0.77$) was obtained when plotting the residual turbidity against phosphorus removal for all polymers and doses (not shown), demonstrating that the residual turbidity decreased when P removal increased and more specifically that P removal can be optimised by improving colloids capture.

3.3. Polymer properties and comparison to performance

The cationic polymers were all defined by the manufacturers as high molecular weight and have measured apparent viscosities of 113.4, 127.1 and 68.7 mPa.s for C1, C2 and C3, respectively when used at a shear rate of 6 /s (Table 2). Less information was available for the anionic polymers where A2 was described as a medium molecular weight and A3 as an ultra-high molecular weight polymer. The corresponding apparent viscosities at a shear rate of 6 /s were 57.7, 182.7, 17.9 and 28.8 mPa.s for A1, A2, A3 and A4, respectively. All the anionic polymers were described as low or low-medium charge and had measured zeta potentials at pH 7.4 of -17.4, -43.6, -12.5, and -7.5 mV for A1, A2, A3 and A4, respectively (Table 2). Measurement of the zeta potential across a pH spectrum revealed that only polymers A1 and A2 had a degree of acid dissociation where the zeta potential becomes more negative as the pH was increased up to around a pH of 5-6 (Supplementary information, Figure S1). The other anionic polymers (A3 and A4) showed only marginal increase in zeta potential as the pH was increased, demonstrating that their charges were predominately fixed in nature. In comparison, the cationic polymers were described as more charged with corresponding zeta potential values at pH 7.4 of 17.4, 32.7 and

16.4 mV at a dose of 1 mg/L. C1 and C2 demonstrated an amphoteric dissociation whereby the zeta potential changed as a function of pH and crossed the zero charge line at pHs of 9.8 and 10.1, respectively. In contrast, C3, exhibited a stable zeta potential over acidic pH which then reduced under alkaline conditions to cross the zero charge line at pH 9.8. Most of the polymers were described as conforming to a linear structure (A2, A3, C1 and C3) with C2 cross-linked and A1 and A4 of unknown structure. The main functional groups were identified to be acrylamide carbonyl, acrylic carbonyl and quaternary ammonium, ester and ether (Figure 8).

All of these except of the latter one (ether) belong to regular cationic or anionic polyacrylamides (Bolto and Gregory, 2007). The ether group peak (72 ppm) was only linked to A2 and A3. The polymers A4 and A1 had no ether group peak assigned to them and both had a similar NMR spectrum. In the group of the cationic polymers, all had strong peaks between 53.9 and 56.3 ppm which could be attributed to quaternary ammonium groups which would confirm the cationic charge of the polymers (Tables 2 and 4). The peak ratios, obtained from integration of the peak area, show big differences in structural composition between the polymers yet complete examination of the chemical structures was not possible due to their complexity. The addition of polymer contributed considerably to P removal performance as was shown with varied combinations of components of the BCP and only combination of all three –coagulant, ballast, polymer– achieved the highest P removal (Figure 2). Experiments on the individual components revealed that the polymer does not act as the primary precipitating agent and so its function related more to the effective incorporation of the ballast into the precipitated aggregate formed by the addition of coagulant. Further, the magnetite does not contribute significantly to phosphorus removal. This is observed through the direct experiment and the comparison of fresh and reused ballast. This is expected as magnetite is a spinel crystal structure with a formula of $\text{Fe}^{+II} \text{Fe}_2^{+III} \text{O}_4$ with the majority of Fe ions at their highest oxidation state (+III). In other cases where iron is used as an adsorbent for phosphorus such as hybrid ion exchange resins, iron ions are in their lower oxidation state +II which is more favourable for adsorption (Anderson and Priestley, 1983; Zi-li et al., 2004; Martin et al., 2009). The assessment of the impact of polymer selection and dose has indicated that phosphorus removal performance in a ballasted flocculation system is best served

with anionic polymers. Whilst this implies the predominant mechanism is not likely to be electrostatic, the presence of calcium ions in the water are known to act as bridging ions (Rabiee, 2010). Furthermore, the recommended polymer dose of 1 mg/L could not be justified with these experiments as doses as low as 0.01 mg/L were shown to be effective and as seen in the cases of C1 and C2, polymer addition can lead to lower phosphorus removal than adding coagulant alone (Figure 3). However, the dose did impact the flocs characteristics with higher doses leading to larger flocs and lower residual turbidity. In such cases, bridging mechanisms are likely to be important and these are best served by large MW linear polymers (Bolto and Gregory, 2007). The poorer removal and smaller floc sizes achieved with C2 supports this due to its crosslinked structure. The enhancement with anionic polymer may also reflect the stronger influence of bridging as direct electrostatic connections will not be made, instead favouring patchwork bridging (Bache and Gregory, 2007). Overall the work has outlined that effective tertiary ballasted flocculation for phosphorus removal is best served with low doses of medium to large MW linear anionic polymers.

4. Conclusions

The results of this work have shown that the complete BCP system achieves higher P removal when compared to coagulant alone and within shorter time frames. However, when cross-comparing the polymers it appeared that cationic polymers C1 and C2 resulted in worse P removal than the anionic A1 and A2. At varying polymer doses, overall performance did not deteriorate much even at doses as low as 0.01 mg/L and therefore the general guidance on using doses of 1 mg/L cannot be supported. Nevertheless, P removal was dependent of polymer dose at a lower coagulant dose which indicated towards a mutual relationship between polymer and coagulant doses with potential to save on both chemicals. When it comes to floc properties, higher polymer doses resulted in larger flocs, lower turbidity and lower fractal dimension values which points towards more open flocs that are potentially better at sweeping particles. When looking at floc breakage rates, it appears that there might be an ideal floc size at which the floc strength is

sufficient enough for achieving excellent P removal. Rather than being a precipitating agent, polymers seem to be acting as the connection between coagulant-wastewater flocs and the ballast particles. These flocs are much weaker compared to coagulant alone (0.8 FS) but strength does not seem to be the crucial factor for efficiency in wastewater treatment (at very short contact times). The guidance that can be taken from this work is that anionic polymers work best in high alkalinity wastewaters (>130 mg CaCO_3/L) when they are at doses below 1 mg/L and coagulant dose between 5-8 mg Fe/L which can achieve more than 90% P removal.

Acknowledgements

Funding for this study was gratefully received from Severn Trent Water. The authors also gratefully acknowledge the supply of the polymers by Kemira, BASF and Goldcrest.

References

- Anderson, N. J., Priestley, A. J., 1983. Colour and turbidity removal with reusable magnetite particles-V: Process Development. *Water Research* 17(10), 1227-1233.
- Bache, D. H., Gregory, R., 2007. *Flocs in Water Treatment*. First edition. IWA Publishing, London, UK.
- Bolto, B. A., Dixon, D. R., Gray, S. R., Chee, H., Harbour, P. J., Ngoc, L., Ware, A. J., 1996. The use of soluble organic polymers in waste treatment. *Water Science and Technology* 34(9), 117-124.
- Bolto, B., Gregory, J., 2007. Organic polyelectrolytes in water treatment. *Water Research* 41(11), 2301-2324.
- Bratby, J., 2016. *Coagulation and Flocculation in Water and Wastewater Treatment - Second Edition*. Volume 3. IWA Publishing, London, UK.
- De Barbadillo, C., Shellswell, G., Cyr, W., Edwards, B., Waite, R., Mullan, J., Mitchell, R., 2010. Pilot testing of four tertiary phosphorus removal processes to achieve ultra-low phosphorus limits at the Lakeshore WPCP in the town of Innisfil , Ontario. *WEFTEC*, Black & Veatch, 1-10.
- Desjardins, C., Koudjonou, B., Desjardins, R., 2002. Laboratory study of ballasted flocculation. *Water Research* 36(3), 744-754.
- Dixon, D., 1991. The sirofloc process for water clarification. *Water Supply* 9(1), S33-S36.
- EU Water Framework Directive, 2000. 2000/60/EC.
- Gasperi, J., Laborie, B., Rocher, V., 2012. Treatment of combined sewer overflows by ballasted flocculation: removal study of a large broad spectrum of pollutants. *Chemical Engineering Journal* 211-212, 293-301.

Ghamen, A. V., Young, J. C., Edwards, F. G., 2007. Mechanisms of ballasted floc formation. *Journal of Environmental Engineering* 133(3), 271-277.

Hook, G., Ott, R., 2001. The Ultimate Challenge for Technology: 0.02 mg/L effluent total phosphorus. *Proceedings of the Water Environment Federation* 12, 113-132.

Imasuen, E., Judd, S., Sauvignet, P., 2004. High-rate clarification of municipal wastewaters: a brief appraisal. *Journal of Chemical Technology and Biotechnology* 79(8), 914-917.

Jarvis, P., Jefferson, B., Gregory, J., Parsons, S., 2005a. A review of floc strength and breakage. *Water Research* 39(14), 3121-3137.

Jarvis, P., Jefferson, B., Parsons, S. A., 2005b. Breakage, regrowth, and fractal nature of natural organic matter flocs. *Environmental Science & Technology* 39(7), 2307-2314.

Jarvis, P., Parsons, S. A., Henderson, R., Nixon, N., Jefferson, B., 2008. The practical application of fractal dimension in water treatment practice - the impact of polymer dosing. *Separation Science and Technology* 43(7), 1785-1797.

Lapointe, M., Barbeau, B., 2019. Substituting polyacrylamide with an activated starch polymer during ballasted flocculation. *Journal of Water Process Engineering* 28, 129-134.

Lapointe, M., Barbeau, B., 2018. Selection of media for the design of ballasted flocculation processes. *Water Research* 147, 25-32.

Lapointe, M., Barbeau, B., 2016. Characterisation of ballasted flocs in water treatment using microscopy. *Water Research* 90, 119-127.

Lee, R. M., Carlson, J. M., Bril, J., Cramer, J., Harenda, J., 2015. Pilot testing reveals alternative methods to meet Wisconsin's low level phosphorus limits". *Proceedings of the Annual WEFTEC National Conference*, 3238-3252.

Zi-li, H., Yue-hua, H., Jing, X., Chun-hua, Z., 2004. Removal of phosphate from municipal sewage by high gradient magnetic separation. *Journal of Central South University of Technology* 11(4), 391-394.

Martin, B. D., Parsons, S. A., Jefferson, B., 2009. Removal and recovery of phosphate from municipal wastewaters using a polymeric anion exchanger bound with hydrated ferric oxide nanoparticles. *Water Science and Technology* 60(10), 2637-2645.

Rabiee, A., 2010. Acrylamide-based anionic polyelectrolytes and their applications: a survey. *Journal of Vinyl and Additive Technology* 21(2), 111-119.

Ragsdale, D., 2007. Advanced wastewater treatment to achieve low concentration of phosphorus. Technical report, Seattle: US EPA.

Sharma, B. R., Dhuldhoya, N. C., Merchant, U. C., 2006. 1) Flocculants - an ecofriendly approach. *Journal of Polymers and the Environment* 14(2), 195-202.

Yeoman, S., Stephenson, T., Lester, J. N., Perry, R., 1988. The removal of phosphorus during wastewater treatment: a review. *Environmental Pollution* 49(3), 183–233.

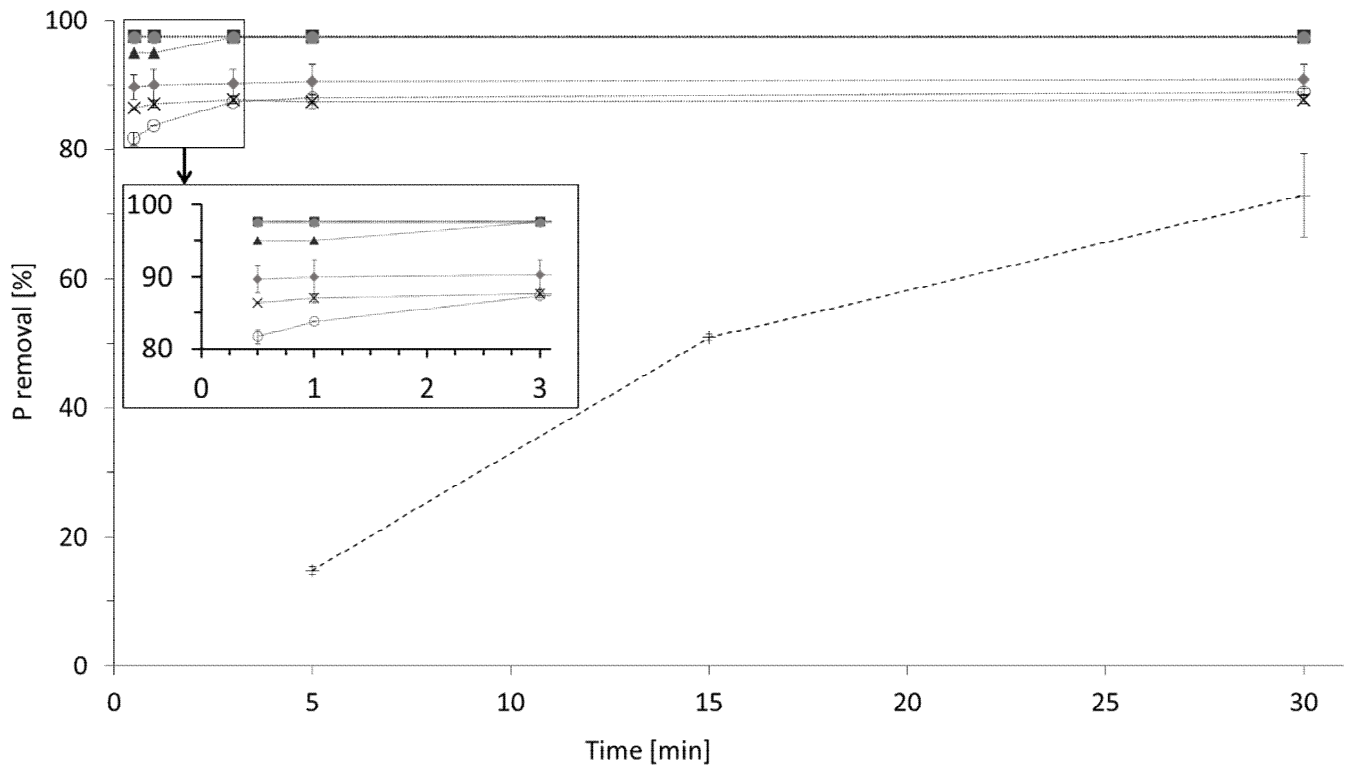


Figure 1: P removal from initial 1 mg P/L in relation to settling time between 0.5 and 30 minutes at 5 mg Fe/L and 0.5 mg/L polymer dose and 5 g/L used magnetite. Polymers: A1 (■), A2 (▲), A3 (x), A4 (□), C1 (◆), C2 (○), and C3 (●) and coagulant only (+).

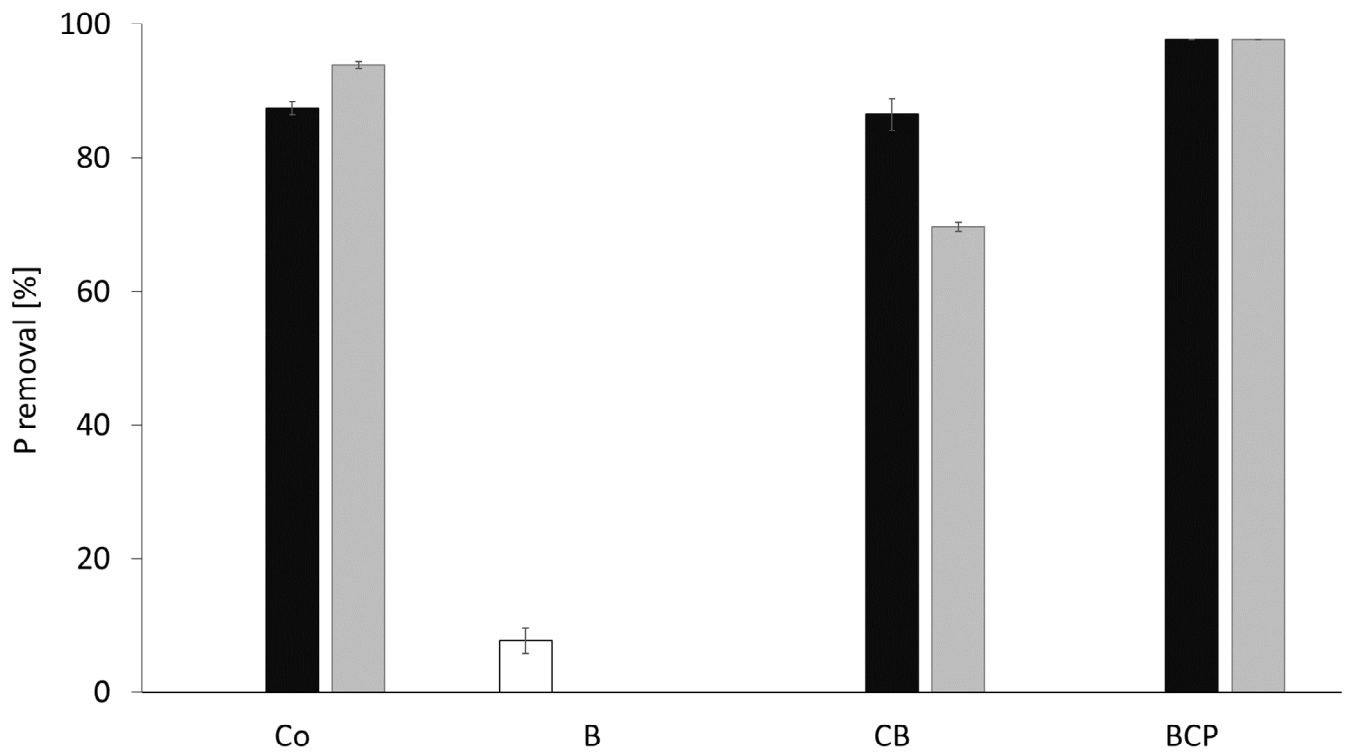


Figure 2: P removal from initial 1 mg P/L with coagulant only (Co), ballast only (B), combination of coagulant and ballast (CB) and all components (BCP, 1 mg/L A1 polymer dose) at 0 mg Fe/L (□) (i.e. tests with no coagulant), 5 mg Fe/L (■) and 8 mg Fe/L (■) after 5 minutes of settling with filtered samples over 0.45 μm .

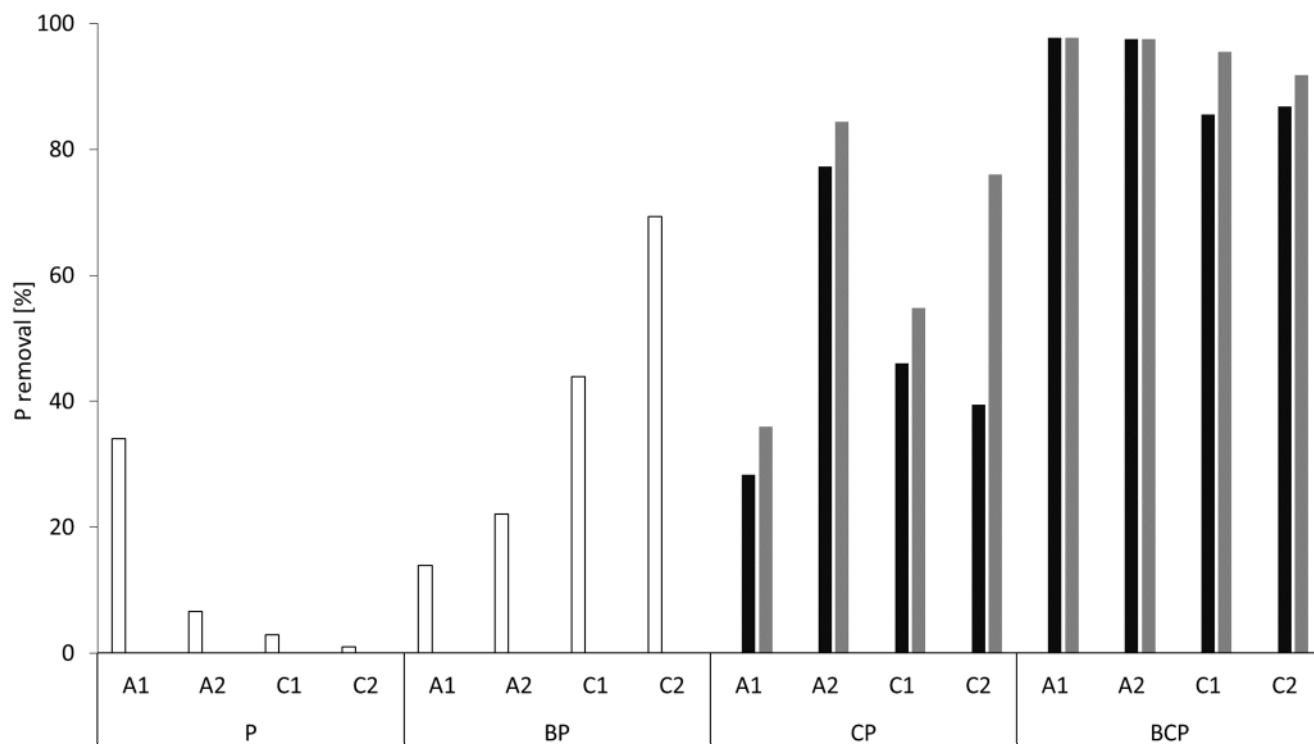
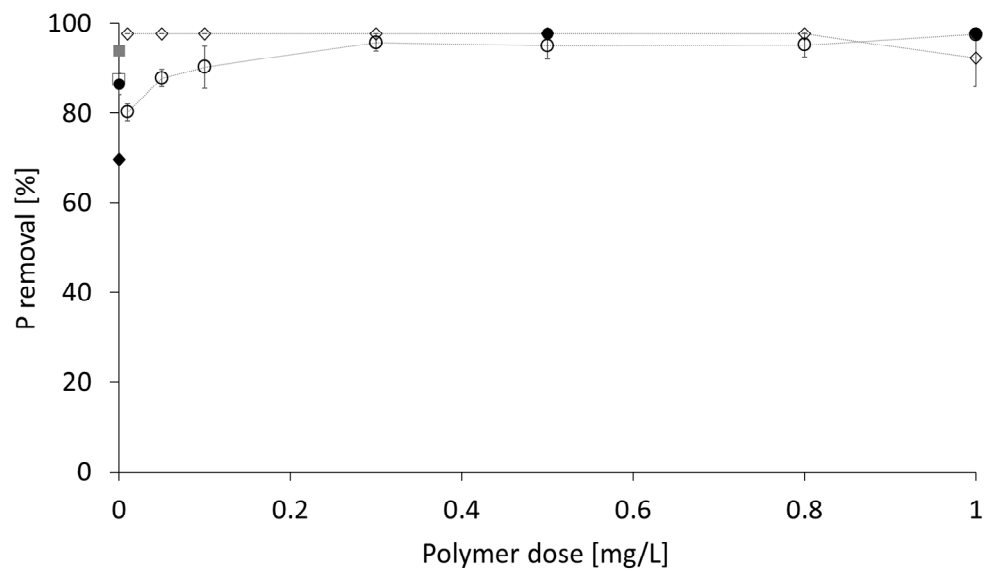
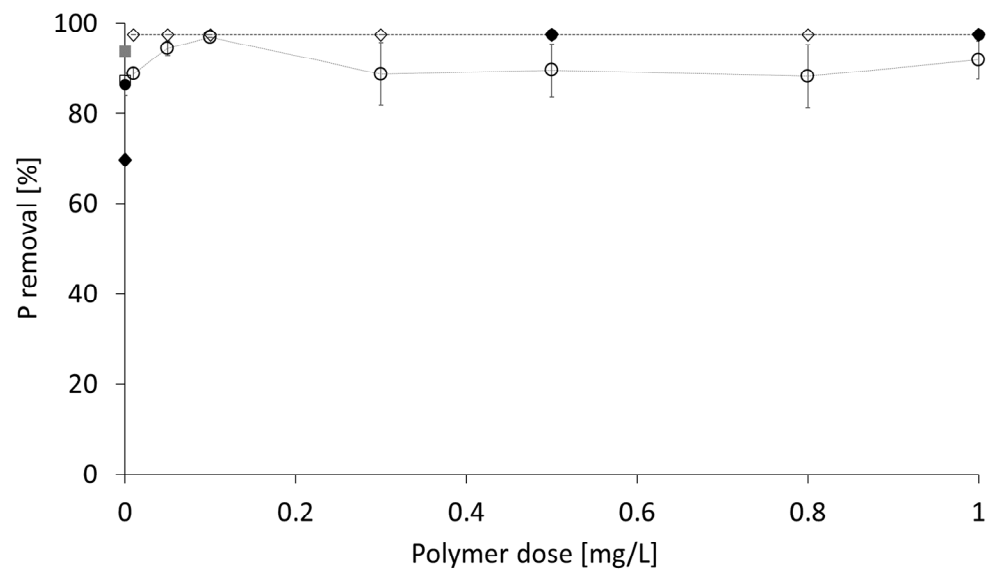


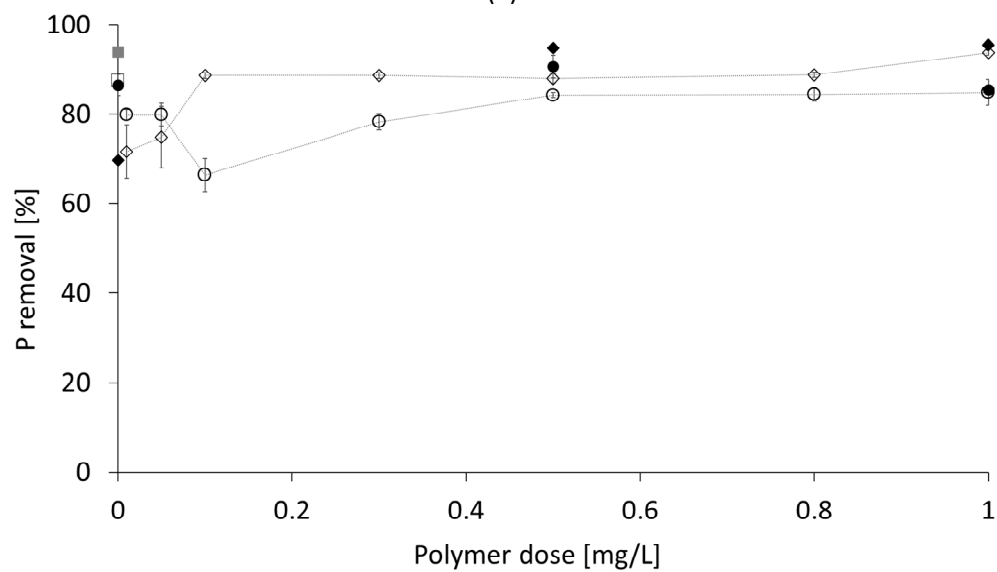
Figure 3. P removal from initial 1 mg P/L at different coagulation combinations: polymer only (P), ballast and polymer (BP), coagulant and polymer (CP), coagulant, ballast and polymer (BCP). Coagulant doses: 0 mg Fe/L (□), 5 mg Fe/L (■) and 8 mg Fe/L (▒), polymer dose: 1 mg/L, ballast (used) dose: 5 g/L, settling time: 5 minutes and filtration over 0.45 μm .



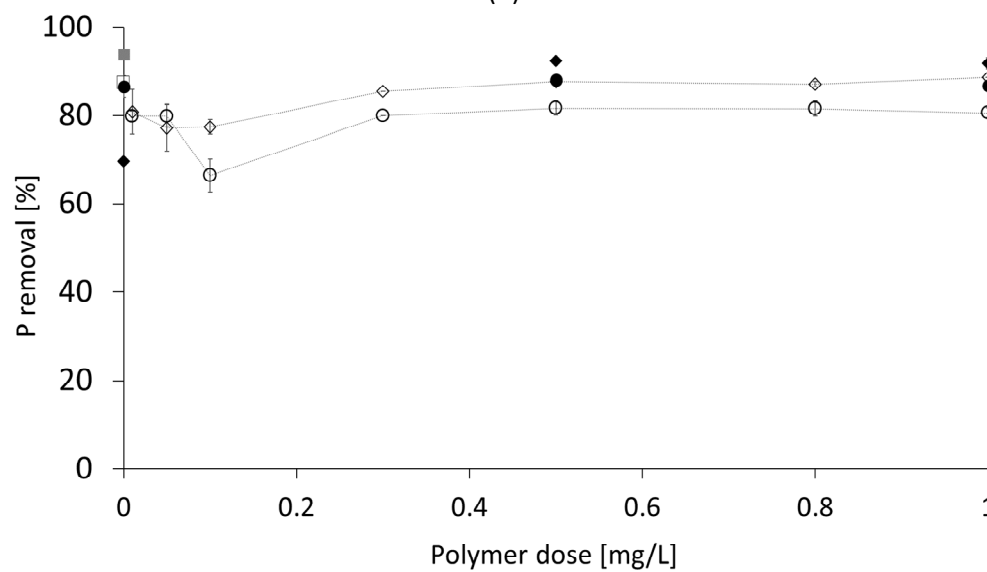
(a)



(b)



(c)



(d)

Figure 4. Polymer dose response curves after 5 minutes of settling time at 5 mg Fe/L with fresh magnetite (○), 8 mg Fe/L with fresh magnetite (◇), at 5 mg Fe/L with used magnetite (●) and 8 mg Fe/L with used magnetite (◆) for (a) A1, (b) A2, (c) C1, (d) C2. In comparison to coagulant only at 5 mg Fe/L (□) and 8 mg Fe/L (■).

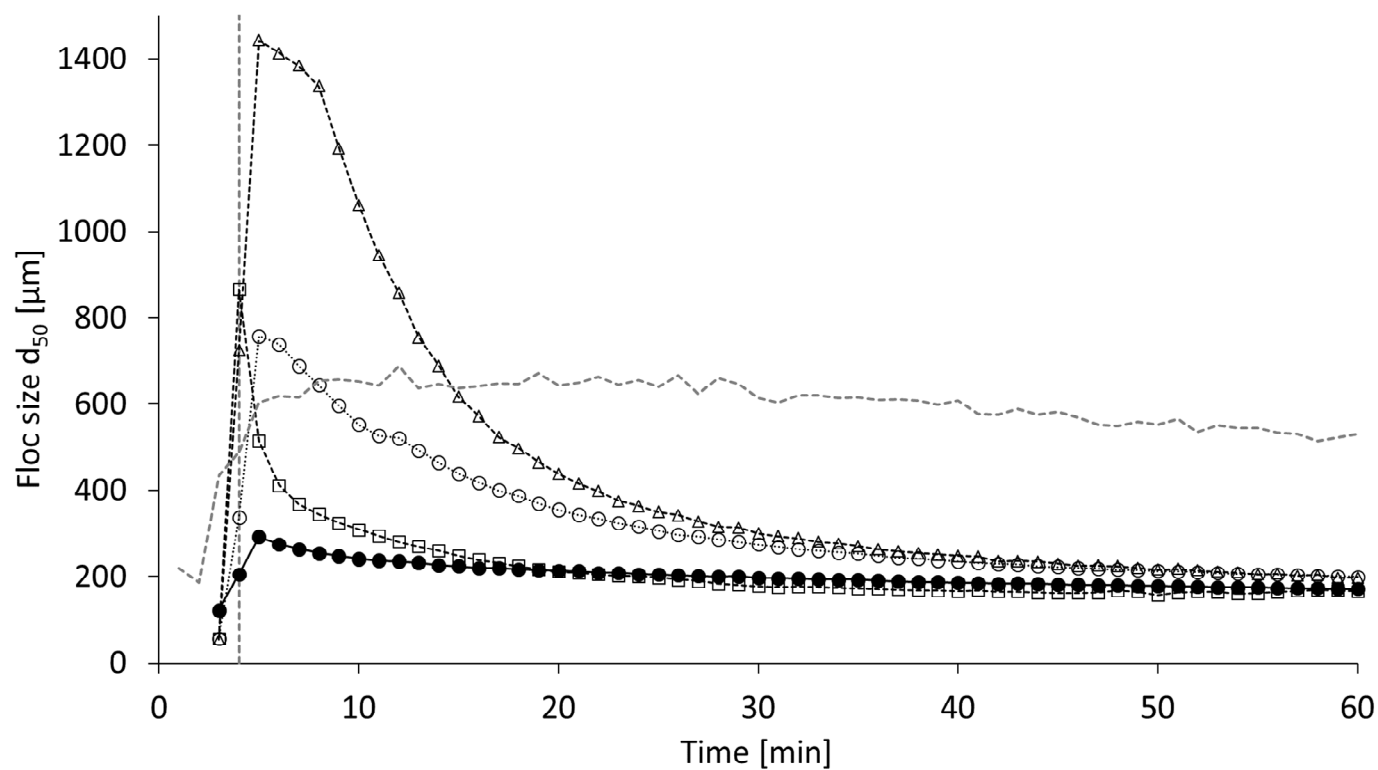


Figure 5. Floc growth with time at 8 mg Fe/L, 5 g/L fresh magnetite and 1 mg/L polymer dose. Polymers: A1 (○), A2 (Δ), C1 (□), C2 (●), coagulant only: ----- . Vertical dotted line indicates 4 minutes, i.e. time when stirring was stopped in jar test procedure.

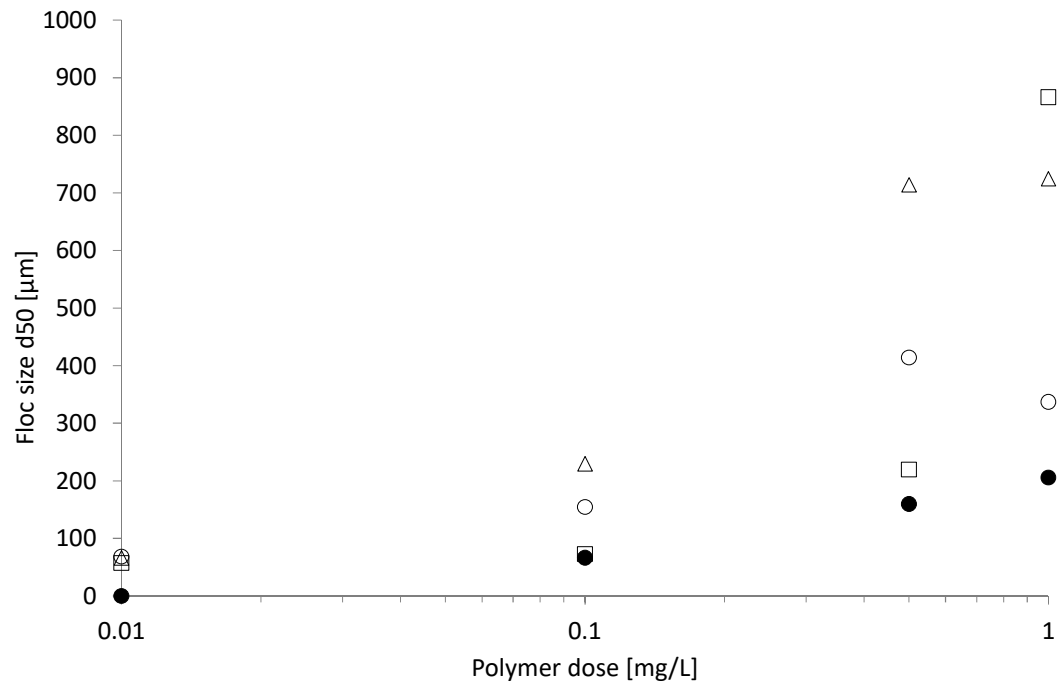
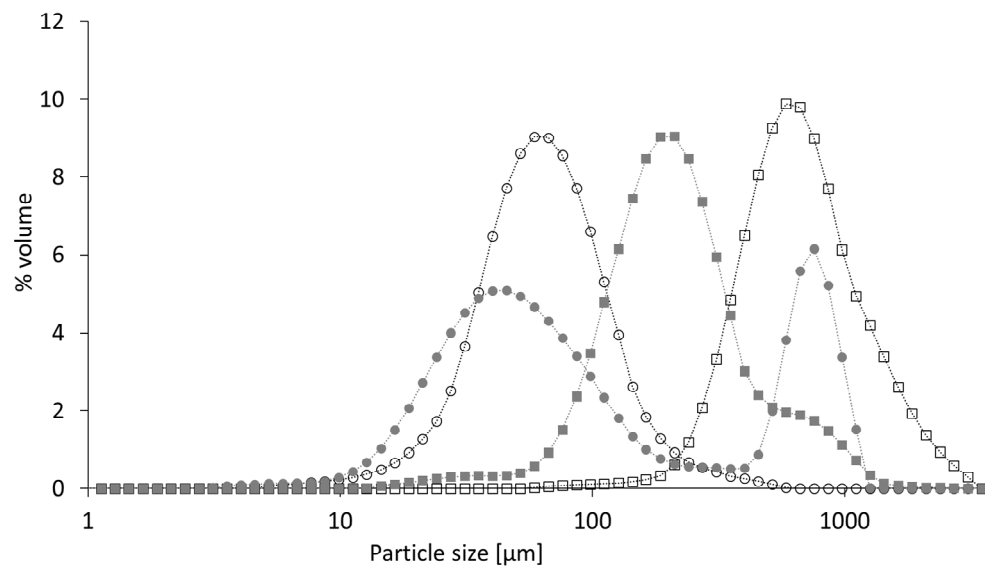
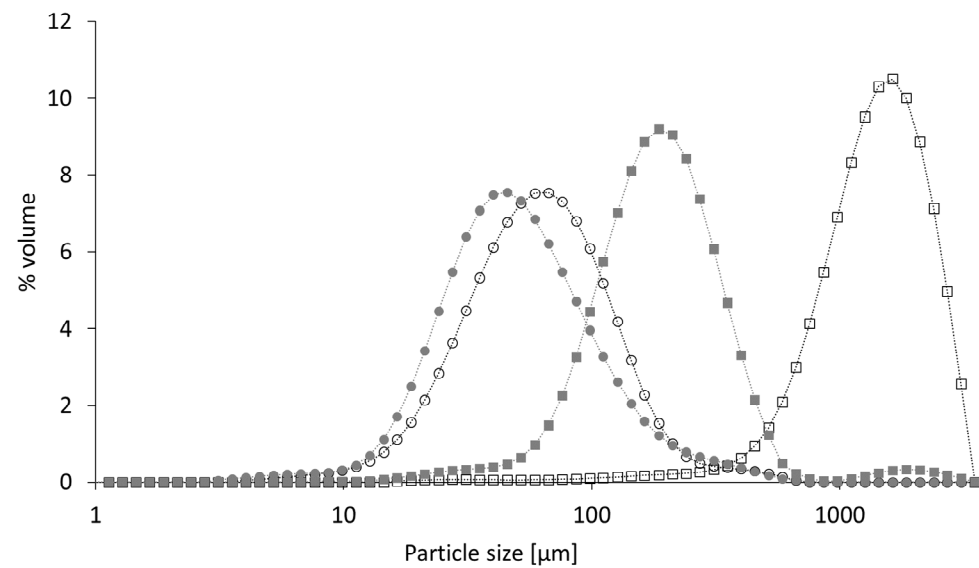


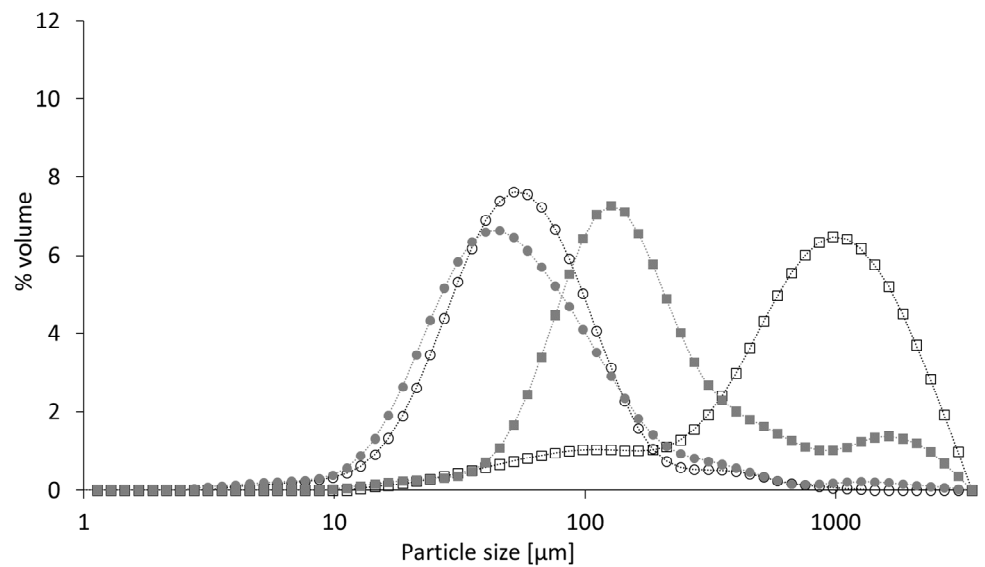
Figure 6. Impact of polymer dose on floc size (d_{50}) after 4 minutes of stirring. All at coagulant dose of 8 mg Fe/L, fresh magnetite dose of 5 g/L and mixing at 200 rpm.



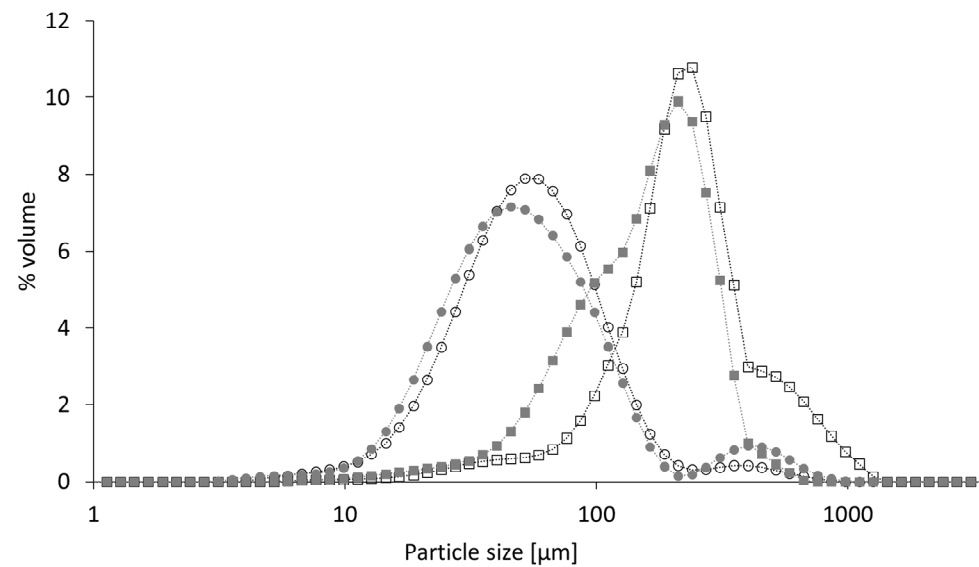
(a)



(b)

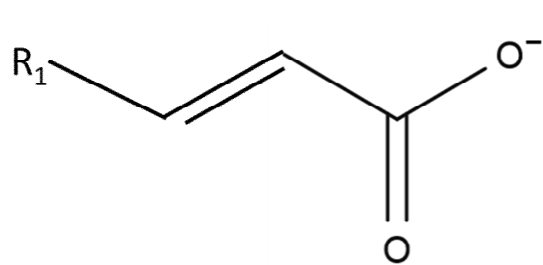


(c)

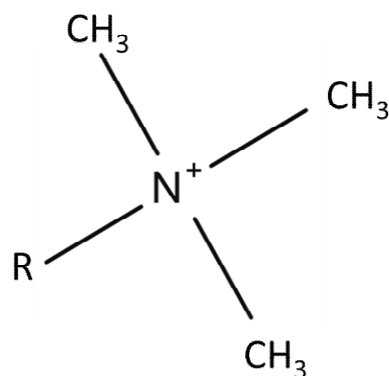


(d)

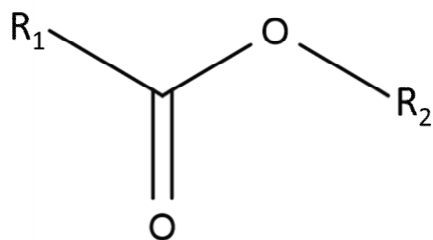
Figure 7. Particle size distribution with 8 mg Fe/L and 5 g/L fresh magnetite. Peak floc size at polymer doses 0.01 mg/L (○) and 1 mg/L (□) and stable floc size (60 min) at 0.01 mg/L (●) and 1 mg/L (■) for polymers (a) A1, (b) A2, (c) C1, (d) C2.



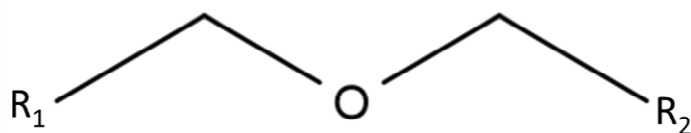
Acrylic carboxyl



Cationic quaternary ammonium



Ester



Ether

Figure 8. Functional groups identified from FTIR and NMR analysis.

Table 1: Wastewater characteristics.

| | COD [mg/L] | Total P [mg/L] | ortho-P [mg/L] | Suspended solids [mg/L] | Alkalinity [mg CaCO ₃ /L] | pH | Zeta potential [mV] near pH 7.4 | Turbidity |
|------------------------------------|-----------------|-------------------|-------------------|-------------------------------|--|----------------|---|----------------|
| Average ± standard deviation | 21.25 ± 2.77 | 1.21 ± 0.36 | 1.09 ± 0.38 | 7.27 ± 3.42 | 178.08 ± 16.34 | 7.42 ± 0.17 | -11.01 ± 1.40 | 2.45 ± 0.88 |
| Number of samples (n) | 78 | 66 | 79 | 76 | 15 | 79 | 9 | 44 |

Table 2: Characteristics of the polymers used in this study (Information as given by suppliers unless otherwise noted).

| Polymer | Charge | Degree of charge | Molecular weight | Apparent viscosity* [mPa.s] at 6s ⁻¹ shear rate | Zeta potential* [mV] near pH 7.4 | Chemical structure |
|---------|----------|------------------|------------------|--|----------------------------------|--------------------|
| A1 | anionic | low | NA | 57.7 | -17.4 ± 10.1 | NA |
| A2 | anionic | low-medium | medium | 182.7 | -43.6 ± 10.0 | linear |
| A3 | anionic | low | ultra-high | 17.9 | -12.5 ± 6.9 | linear |
| A4 | anionic | low | NA | 28.8 | -7.5 ± 2.5 | NA |
| C1 | cationic | low-medium | very high | 113.4 | 17.4 ± 4.6 | linear |
| C2 | cationic | high | very high | 127.1 | 32.7 ± 1.5 | cross-linked |
| C3 | cationic | medium | very high | 69.7 | 16.4 ± 6.2 | linear |

*: measured, NA: not available

Table 3. P removal and turbidity after 5 minutes of settling. Floc sizes and fractal dimensions (D_f) after 4 minutes of stirring. Floc strength factor (FS) based on d_{50} peak and stable sizes. All at coagulant dose of 8 mg Fe/L, fresh magnetite of 5 g/L and mixing at 200 rpm.

| Polymer | Dose [mg/L] | P removal [%] | Turbidity [NTU] | d_{50} [μm] | d_{10} [μm] | Mode [μm] | D_f | FS |
|---------|-------------|----------------|-----------------|----------------------------|----------------------------|------------------------|-------|------|
| A1 | 0.01 | 97.6 ± 0 | 1.8 | 68.3 ± 8.3 | 31.1 ± 3.1 | 71.6 ± 9.8 | 2.7 | 0.73 |
| | 0.1 | 97.6 ± 0 | 1.0 | 154.3 ± 7.5 | 49.5 ± 4.2 | 195.3 ± 32.9 | 2.6 | 0.42 |
| | 0.05 | 97.6 ± 0 | 0.8 | 413.7 ± 204.9 | 89.8 ± 41.2 | 411.7 ± 381.7 | 2.2 | 0.24 |
| | 1 | 92.2 ± 6.3 | 0.9 | 337.0 ± 17.8 | 69.0 ± 9.6 | 583.0 ± 86.1 | 2.3 | 0.26 |
| A2 | 0.01 | 97.4 ± 0 | 1.7 | 66.2 ± 7.3 | 27.2 ± 3.1 | 68.1 ± 11.4 | 2.7 | 0.8 |
| | 0.1 | 97.4 ± 0 | 1.4 | 229.3 ± 14.0 | 61.8 ± 3.7 | 316.0 ± 16.0 | 2.6 | 0.32 |
| | 0.05 | 97.4 ± 0 | 0.7 | 714.0 ± 120.4 | 90.2 ± 15.4 | 974.7 ± 307.0 | 2.5 | 0.12 |
| | 1 | 97.4 ± 0 | 0.7 | 724.3 ± 94.2 | 75.9 ± 9.7 | 1476.7 ± 170.1 | 2.2 | 0.14 |
| C1 | 0.01 | 71.6 ± 6.0 | 3.6 | 57.0 ± 4.1 | 24.4 ± 1.7 | 56.5 ± 6.2 | 2.8 | 0.97 |
| | 0.1 | 88.6 ± 0.6 | | 72.6 ± 2.3 | 28.8 ± 2.3 | 73.6 ± 10.1 | 2.7 | 1.15 |
| | 0.05 | 87.9 ± 1.0 | 1.6 | 219.5* | 56.8* | 299.0* | 2.6 | 0.62 |
| | 1 | 93.7 ± 0.6 | 1.1 | 866.0 ± 99.0 | 139.0 ± 20.7 | 1070.0 ± 177.2 | 2.5 | 0.19 |
| C2 | 0.01 | 80.9 ± 5.1 | 2.3 | 59.0 ± 6.4 | 25.0 ± 2.3 | 61.2 ± 9.3 | 2.8 | 0.9 |
| | 0.1 | 77.5 ± 1.7 | 3.6 | 66.4 ± 4.3 | 24.8 ± 2.0 | 65.4 ± 7.8 | 2.7 | 1.24 |
| | 0.05 | 87.7 ± 0.6 | 1.6 | 159.5 ± 29.5 | 45.6 ± 5.7 | 231.7 ± 118.0 | 2.5 | 0.41 |
| | 1 | 88.6 ± 0 | 1.7 | 205.6 ± 98.2 | 92.1 ± 81.0 | 270.7 ± 154.1 | 2.3 | 0.59 |

*No standard deviation as only two measurements were done.

Table 4: Peak ratios for functional groups determined from ^{13}C -NMR.

| Polymer Chemical shift [ppm] | Degree of charge | Acrylic carbonyl group 185-186 | Acrylamide carbonyl 182, 44-45, 37 | Ether 72 |
|------------------------------------|------------------|--|--|------------------------|
| A1 | Low | 0.1 | 0.3 | |
| A2 | Low-medium | 0.15 | 0.28 | 0.09 |
| A3 | Low | 2.2 | 19.5 | 8 |
| A4 | Low | 0.2 | 1 | |
| | | Cationic quaternary ammonium 53.9-56.3 | Acrylamide carbonyl 179-182, 41.5-45, 34- 37 | Ester 175-177, 64.2 |
| C1 | Low-medium | 1 | 1.4 | 0.4 |
| C2 | High | 1 | 1.4 | 8.6 |
| C3 | Medium | 1.53 | 0.4 | 2.62 |